Proceeding of the 2004 American Control Conference
Boston, Massachusetts June 30 - July 2, 2004

Model-Based Broken Rotor Bar Detection on an IFOC Driven Squirrel Cage Induction Motor

Hugo Rodríguez-Cortés, Christoforos N. Hadjicostis and Aleksandar M. Stanković

Abstract— **In this paper, we propose an on-line monitoring scheme to detect broken rotor bars on IFOC driven squirrel cage induction motors. The drive's variable speed nature complicates the use of classical spectrum analysis techniques. The proposed model-based monitoring scheme does not rely on spectral methods; instead, it monitors, a carefully selected induction motor state, using an on-line observer. The key to fault detection is the development of a simplified dynamic model of a squirrel cage induction motor with broken rotor bars, and the selection, based on techniques from differential geometric theory, of the induction motor state to monitor. Numerical simulations of very different motors validate the model and the monitoring scheme.**

I. INTRODUCTION

Induction motors are the dominant component in industrial processes involving electromechanical energy conversion; thus, they consume between 40 to 50 % of the electric energy in industrialized nations. Safety, reliability and efficiency are major concerns in modern induction motor applications. For these reasons, in the past years there has been an increased interest into induction motor fault detection and diagnosis.

Experience has shown that broken rotor bars can be a serious problem with certain induction motors with arduous work cycles. Although broken rotor bars do not initially cause an induction motor to fail, they can have serious secondary effects. The fault may result in broken parts of the bar hitting stator windings at high velocity. This can cause a serious damage to the induction motor; therefore, faulty rotor bars need to be detected as early as possible.

Broken rotor bars cause disturbances of the flux pattern in induction machines. These non-uniform magnetic field components affect machine torque and stator terminal quantities and are thus detectable by monitoring schemes. To date, different methods have been proposed for broken rotor bar detection. The most well known approach is the non-model-based Motor Current Signature Analysis (MCSA) method [1]. This method monitors, in the frequency domain, sideband components around the fundamental component of stator currents. The main disadvantage of the MCSA method is that it relies on the interpretation of the frequency components of the stator current spectrum, which are influenced by many factors, including electric supply, and static and dynamic load conditions. These conditions may lead to errors in the fault detection task [2]. On the other hand, a practical advantage of MCSA is that only stator currents need to be measured. Fuzzy logic [3] and neural networks [4] techniques have been proposed to handle load-related ambiguous frequency components. The MCSA method has been the main approach used for detecting broken rotor bars on induction motors operating in open-loop; however, spectral analysis techniques applicable under variable speed conditions have also been presented in the literature (for instance in [5] and [6]).

In spite of the extensive work on broken rotor bar detection, model-based techniques have not received much attention. Main reasons are that fault-related induction motor parameters are not well known, and available models are quite complicated to be tractable with model based fault detection techniques. However, by making a compromise between a better tracking of the fault-related signals (by using dynamic models) and a reduced spectrum of validity of the results (due to assumptions about the induction motor parameters), researchers have recently proposed model-based broken rotor bar detection techniques. One such an example is the Vienna Monitoring Method (VMM) presented in [7]. The VMM is based on the comparison of the computed electromechanical torque from two real-time machine models. A healthy induction motor leads to equal values computed by the two models, whereas a non-healthy induction motor excites the models in a different way, leading to a difference between computed torque values. This difference is used to determine the existence of broken rotor bars. The VMM has one disadvantage, which is also present in the proposed monitoring scheme of this paper: variations on the time rotor constant deteriorate the performance of the fault detection scheme.

Among the different approaches for model-based fault detection, geometric methods are of high interest. Geometric theory offers various advantages as it gives a more general formulation of the fault detection problem. However, to date, geometric techniques have not been applied to solve the broken rotor bars detection problem in squirrel cage induction motors.

In this article, we propose a model-based method to detect broken rotor bars on an IFOC driven squirrel cage induction motor. The proposed solution does not rely on spectrum analysis techniques, but monitors instead the output signal of a residual generator that is constructed following the fault detector design presented in [8], [9] and [10]. The rest of the article is organized as follows. Section II presents the simplified model of a squirrel cage induction

H. Rodríguez-Cortés and A. M. Stanković are with the Department of Electrical and Computer Engineering, Northeastern University, Boston, MA, 02115 cortes{astankov}@ece.neu.edu

C. N. Hadjicostis is with the Department of Electrical and Computer Engineering, University of Illinois at Urbana Campaign, Urbana, IL, 61801 chadjic@uiuc.edu

0-7803-8335-4/04/$17.00 ©2004 AACC

motor with broken rotor bars. Section III presents the fault detection technique. Section IV presents the monitoring scheme design. Finally, Section V gives some concluding remarks.

II. SQUIRREL CAGE INDUCTION MOTOR MODEL WITH BROKEN ROTOR BARS

To apply model-based fault detection techniques it is necessary to have models with two important characteristics: simple enough to be tractable and detailed enough to capture the fault effects of interest. With these characteristics in mind, we develop a model less detailed than the models presented, for instance, in [11] and [12], with the particularity that the effect of broken rotor bars is taken into account by adding only one additional state to the classical induction motor model (presented for instance, in [13]); thus, tractability is achieved.

The proposed model is based on the suggestion that the super-imposition of an extra set of rotor currents on those normally found in a healthy motor may simulate the effect of broken rotor bars [11]. Our main assumptions are summarized as follows, see Figure 1.

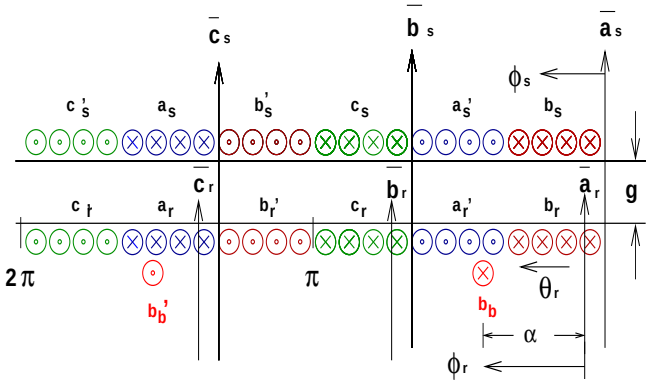

Fig. 1. Developed diagram of the cross-sectional view.

1 Due to high permeability of steel, magnetic fields exist only in the air gap g and have radial direction $\bar{a}_r$, since the air gap is small relative to the inside diameter of the stator.
2 The stator windings $a_s - a'_s$, $b_s - b'_s$ and $c_s - c'_s$ are identical in that each winding has the same resistance r_s and the same number of turns. The rotor windings $a_r - a'_r$, $b_r - b'_r$ and $c_r - c'_r$ are identical in the same sense. All windings have sinusoidal distribution.
3 The extra set of rotor currents (representing the broken bar) is included by adding an extra winding, denoted by $b_b - b'_b$, to the original rotor windings.
4 Magnetic saturation, eddy-currents and friction losses are not included in our analysis.

In Figure 1, $\bar{a}_s$, $\bar{b}_s$, $\bar{c}_s$ and $\bar{a}_r$, $\bar{b}_r$, $\bar{c}_s$ denote the positive direction of the magnetic fluxes produced by each winding. $\otimes$ indicates the positive direction of current. The angular displacement of the rotor relative to $\bar{a}_r$ is denoted by θ_r, the stator angular displacement relative to $\bar{a}_s$ is denoted ϕ_s, while the rotor angular displacement relative to $\bar{a}_r$ axis is denoted ϕ_r. The angular displacements θ_r, ϕ_r and ϕ_s are related as

$$\phi_s = \phi_r + \theta_r.$$

Following the modeling procedure of [13], we have that the dynamic model of a squirrel cage induction motor with broken bars is described by

$$\begin{array}{rcl} \dot{\psi}_{abcs} & = & -R_s\, i_{abcs} + v_{abcs} \\ \dot{\psi}_{abcr} & = & -R_r\, i_{abcr} \\ \dot{\psi}_b & = & -r_b\, i_b, \end{array} \tag{1}$$

where ψ_{abcs}, ψ_{abcr}[1] are the stator and rotor flux linkages, i_{abcs}, i_{abcr} are the stator and rotor currents, v_{abcs} are the stator voltages, ψ_b, i_b are the broken bar related flux linkage and current, $R_r = \text{diag}\{r_r\}$ is the rotor resistance matrix, with r_r the rotor winding resistance, and $R_s = \text{diag}\{r_s\}$ is the stator resistance matrix. Flux linkages and currents are related as

$$\begin{bmatrix} i_{abcs} \\ i_{abcr} \\ i_b \end{bmatrix} = \begin{bmatrix} \mathbf{L}_s & \mathbf{L}_{sr} & \mathbf{L}_{bs} \\ \mathbf{L}_{sr}^\top & \mathbf{L}_r & \mathbf{L}_{br} \\ \mathbf{L}_{bs}^\top & \mathbf{L}_{br}^\top & \mathbf{L}_b \end{bmatrix} \begin{bmatrix} \psi_{abcs} \\ \psi_{abcr} \\ \psi_b \end{bmatrix}, \tag{2}$$

where

$$\begin{array}{rcl} \mathbf{L}_{bs} & = & L_{bs} \begin{bmatrix} \cos(\theta_\beta) & \cos(\theta_\beta - c) & \cos(\theta_\beta + c) \end{bmatrix}, \\ \mathbf{L}_{br} & = & L_{br} \begin{bmatrix} \cos(\alpha) & \cos(\alpha - c) & \cos(\alpha + c) \end{bmatrix}, \\ \mathbf{L}_s & = & \begin{bmatrix} L_{ls} + L_{ms} & -\frac{1}{2} L_{ms} & -\frac{1}{2} L_{ms} \\ -\frac{1}{2} L_{ms} & L_{ls} + L_{ms} & -\frac{1}{2} L_{ms} \\ -\frac{1}{2} L_{ms} & -\frac{1}{2} L_{ms} & L_{ls} + L_{ms} \end{bmatrix}, \\ \mathbf{L}_r & = & \begin{bmatrix} L_{lr} + L_{mr} & -\frac{1}{2} L_{mr} & -\frac{1}{2} L_{mr} \\ -\frac{1}{2} L_{mr} & L_{lr} + L_{mr} & -\frac{1}{2} L_{mr} \\ -\frac{1}{2} L_{mr} & -\frac{1}{2} L_{mr} & L_{lr} + L_{mr} \end{bmatrix}, \\ \mathbf{L}_{sr} & = & L_{sr} \begin{bmatrix} \cos(\theta_r) & \cos(\theta_r + c) & \cos(\theta_r - c) \\ \cos(\theta_r - c) & \cos(\theta_r) & \cos(\theta_r + c) \\ \cos(\theta_r + c) & \cos(\theta_r - c) & \cos(\theta_r) \end{bmatrix} \end{array} \tag{3}$$

with $\theta_\beta = \theta_r - \alpha$ and $c = \frac{2\pi}{3}$.

In equations (2) and (3), L_{ls}, L_{ms} are the stator leakage and self inductance, L_{lr}, L_{mr} are the rotor leakage and self inductance, $L_{sr} = L_{ms}$ the stator-rotor mutual inductance, L_{br}, $L_{bs} = L_{br}$ is the broken bar related winding to stator and to rotor mutual inductance respectively, $\mathbf{L}_b$ is the broken bar related winding self inductance and α is the angular position of the broken bar related winding. Finally, the mechanical dynamics is described by

$$J\,\dot{\omega}_m = \tfrac{P}{2} \tfrac{d}{d\,\theta_r} (i_{abcs}^\top\, \mathbf{L}_{sr}\, i_{abcr} + i_{abcs}^\top\, \mathbf{L}_{bs}\, i_b) - \tau_L, \tag{4}$$

where ω_m denotes the mechanical rotor velocity, P the number of poles, J the mechanical inertia and τ_L the load torque.

[1]We consider $f_{abcx} = [\ f_{ax} \quad f_{bx} \quad f_{cx}\ ]^\top$.

Note that the broken bar related winding inductances L_{br} and L_{bs}, the resistance of the broken rotor bar related winding r_b and the angular position α are unknown parameters since it is not possible to know in advance the number and the position of the broken rotor bars.

It is well known that broken bars result on sideband components around the fundamental of the stator currents at frequencies given by [2]

$$f_b \quad = \quad (1 \pm 2s)\, f_s \tag{5}$$

where s is the per unit slip and f_s is the supply frequency. In order to verify that our model has components at those frequencies we performed a numerical simulation applying a $460\,V$, 3-phase balanced voltage. We have considered two induction motors with parameters as follows.

Parameter	Motor 1 ($3HP$)	Motor 2 ($100HP$)
L_{ls}, L_{lr} (H)	0.024, 0.013	0.0004, 0.0006
L_{ms} (H)	0.245	0.0096
r_r, r_s (Ω)	1.34, 1.77	0.037, 0.025
P	4	4
J $(kg\,m^2)$	0.025	0.863
τ_L(Nm)	12	90

Concerning the broken rotor bar parameters, experimental evidence has shown that when the amplitude of the broken rotor bar harmonics (5) is over $50\,dB$ smaller than the fundamental frequency component amplitude, the rotor may be considered healthy [14]. In order to simulate a non healthy induction motor we choose the fault related parameters as shown in the table below.

Parameter	Motor 1 ($3HP$)	Motor 2 ($100HP$)
$L_{bs} = L_{br}$ (H)	0.0045	0.00043
$\mathbf{L}_b$ (H)	0.0046	0.00047
r_b (Ω)	0.015	0.043

With the selected parameters we have for motor 1 $s = 0.0166$ and $f_b = \{58.04, 61.95\}$, while for motor 2 we have $s = 0.024$ and $f_b = \{59.71, 60.29\}$. As observed in Figure 2, the stator current has components at those frequencies with amplitude corresponding to a non-healthy induction motor.

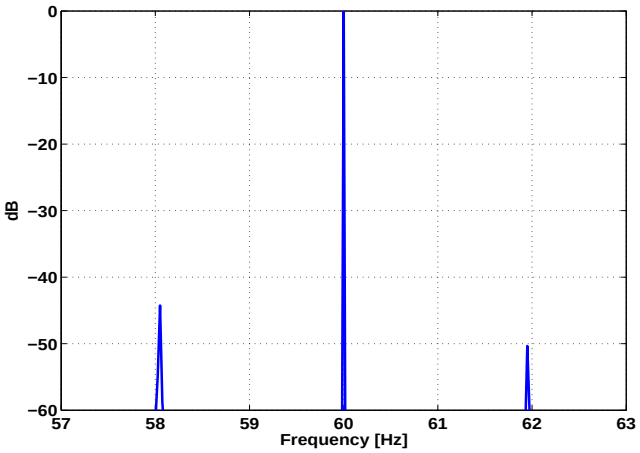

Motor 1

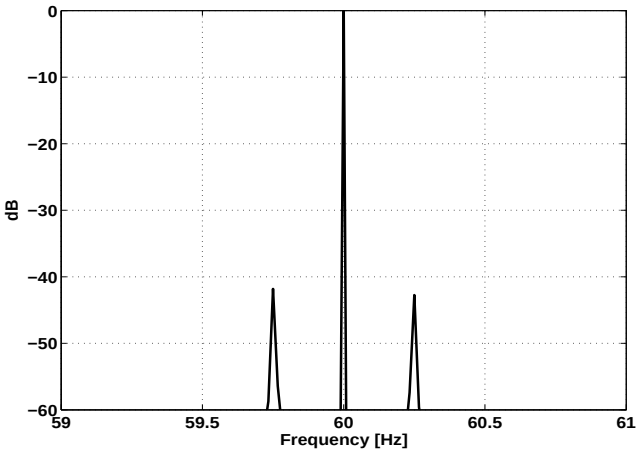

Motor 2

Fig. 2. Spectral content of stator current i_{as}.

III. MODEL BASED FAULT DETECTOR DESIGN

The general procedure of fault detection, isolation and accommodation (FDIA) in dynamic systems with the aid of analytical redundancy consists of the following three-step [18]:

(a) Generation of functions that carry information about the faults, so-called residuals;
(b) Decision on the occurrence of a fault and localization of the fault, so-called isolation;
(c) And accommodation of the faulty process to normal operation.

This paper focuses attention on the first step.

Residuals are quantities expressing the difference between the actual plant outputs and those expected based on the applied inputs and the mathematical model. These residuals are obtained by exploiting dynamic relationships among sensor outputs and actuator inputs. An important characteristic for residuals is that they need to be robust with respect to the effect of nuisance faults, otherwise nuisance faults will obscure the residual's performance by acting as a source of false alarms complicating the second step of the FDIA procedure.

Much of the work on the generation of residuals has been performed in the analytic redundancy framework and, since the Fault Detection Filter (FDF) of Beard and Jones [15], [16], this problem has attracted great interest. In the LTI setting the residual generation problem was solved by Massoumnia in [9] using an advanced version of the FDF of Beard and Jones. In the nonlinear setting the residual generation problem using analytic redundancy has been addressed in [17] for state-affine systems and lately in [10] for input-affine systems. In these works, residual generator construction is based, under mild assumptions in the nonlinear case, on the existence of an unobservability subspace (distribution) leading to a subsystem unaffected by

all fault signals but the fault of interest; then an asymptotic observer for such a subsystem, which in the nonlinear case may not exist, yields the residual generator.

Consider the following system

$$\begin{aligned} \dot{x} &= f(x) + g(x)\,u + l_n(x)\,m_n + l_t(x)\,m_t \\ y &= h(x); \end{aligned} \tag{6}$$

where $x \in \mathbb{R}^n$ is the state, $y \in \mathbb{R}^k$ is the measurable output, $u \in \mathbb{R}^m$ is the input and $m_t \in \mathbb{R}^{l_1}$, $m_n \in \mathbb{R}^{l_2}$ are arbitrary unknown functions of time, representing the target failure modes and the nuisance failure modes respectively. During fault-free operation they are equal to zero. The columns of $g(x)$, $l_m(x)$ and $l_t(x)$, $f(x)$ and $h(x)$ are smooth vector fields with $l_m(x)$ and $l_t(x)$ denoting the actuator failure signatures.

The residual generation problem may be stated as follows.

Problem 1: Consider the nonlinear system described by (6). Design, if possible, a dynamic residual generator with state $\hat{x} \in R^e$ of the form

$$\begin{aligned} \dot{\hat{x}} &= F(\hat{x}, y) + E(\hat{x}, y)\,u \\ r &= M(\hat{x}, y), \end{aligned} \tag{7}$$

where $F(\hat{x}, y)$ and the columns of $E(\hat{x}, y)$ are smooth vector fields and $M(\hat{x}, y)$ is an smooth mapping, that takes y and u as inputs and generates the residual r with the following local properties:

(i) When the target failure m_t is not present, the residual generator (7) is asymptotically stable and r decays asymptotically to zero, that is, the transmission from the input u and the nuisance faults m_n to the residual is zero.

(ii) For a nonzero target fault, the residual is nonzero.

Condition (i) considers the stability of the residual generator and assures that the input signal u and the nuisance faults m_n do not affect the residual r. Condition (ii) guarantees that the target fault affects the residual.

In [10] a necessary condition for the existence of a solution to Problem 1 is given. This condition, under mild assumptions, leads to a subsystem driven only by the fault of interests. Thus, a solution to Problem 1 can be found provided such a subsystem admits an observer.

Specifically, assume that the minimal unobservability distribution of (6), denoted by $\mathcal{S}^*$, containing the image of the of the nuisance fault signature L_n, i. e. $L_n = \text{span}\{l_n(x)\}$, is locally nonsingular. In [10] it is shown that if

$$\mathcal{S}^* \bigcap \text{span}\{l_t(x)\} = \{0\} \tag{8}$$

then it is possible, under certain conditions, to find a state diffeomorphism and an output diffeomorphism

$$z = \begin{bmatrix} z_1 \\ z_2 \\ z_3 \end{bmatrix} = \Phi(x), \quad \begin{bmatrix} w_1 \\ w_2 \end{bmatrix} = \Psi(y) \tag{9}$$

such that in the new coordinates, the system (6) is described by equations of the form

$$\begin{aligned} \dot{z}_1 &= \tilde{f}_1(z_1, z_2) + \tilde{g}_1(z_1, z_2)\,u + \tilde{l}_{t1}(z)\,m_t \\ \dot{z}_2 &= \tilde{f}_2(z) + \tilde{g}_2(z)\,u + \tilde{l}_{t2}(z)\,m_t + \tilde{l}_{n2}(z)\,m_n \\ \dot{z}_3 &= \tilde{f}_3(z) + \tilde{g}_3(z)\,u + \tilde{l}_{t3}(z)\,m_t + \tilde{l}_{n3}(z)\,m_n \\ w_1 &= \tilde{h}_1(z_1) \\ w_2 &= z_2, \end{aligned}$$

from where it is possible to extract a subsystem driven only by the target fault as

$$\begin{aligned} \dot{z}_1 &= \tilde{f}_1(z_1, w_2) + \tilde{g}_1(z_1, w_2)\,u + \tilde{l}_{t1}(z)\,m_t \\ w_1 &= \tilde{h}_1(z_1). \end{aligned} \tag{10}$$

Clearly when it is possible to construct an observer for (10), Problem 1 is solvable.

The computation of the minimal unobservability distribution $\mathcal{S}^*$ containing L_n can be computed as the last element of the following sequence [10]:

$$\begin{aligned} S_0 &= W^* + \text{Ker}\,\{dh\}, \\ S_i &= W^* + [f, S_{i-1} \bigcap \text{Ker}\,\{dh\}] \\ &\quad + [g, S_{i-1} \bigcap \text{Ker}\,\{dh\}]\,,\ i = 1, \cdots, k, \end{aligned} \tag{11}$$

where $k \leq n-1$ is determined by the condition $S_k = S_{k-1}$. Concerning W^*, it is computed as the last element of the following sequence:

$$\begin{aligned} W_0 &= \overline{P}, \\ W_1 &= \overline{W}_{i-1} + \left[f, \overline{W}_{i-1} \bigcap \text{Ker}\,\{dh\}\right] \\ &\quad + \left[g, \overline{W}_{i-1} \bigcap \text{Ker}\,\{dh\}\right],\ i = 1, \cdots, k, \end{aligned} \tag{12}$$

with $k \leq n-1$ determined by the condition $W_{i+1} = W_i$. In (11) and (12), $[.,.]$ is the Lie product, $\overline{X}$ denotes the involutive closure of X and $P = \text{span}\,\{l_n(x)\}$.

IV. BROKEN ROTOR BAR DETECTION

Next, we design a residual generator to detect broken rotor bars on an IFOC driven squirrel cage induction motor. To this end, by considering i_b as an externally generated signal, we express the induction motor dynamics (6) in terms of a dq frame rotating at synchronous speed ω_e. Thus, we have

$$\begin{aligned} \dot{\psi}_{qs} &= -r_s\,i_{qs} - \omega_e\,\psi_{ds} + v_{qs} \\ \dot{\psi}_{ds} &= -r_s\,i_{ds} + \omega_e\,\psi_{qs} + v_{ds} \\ \dot{\psi}_{qr} &= -\tfrac{1}{\tau_r}\,\psi_{qr} - \omega_s\,\psi_{dr} + \tfrac{L_m}{\tau_r}\,i_{qs} - \tfrac{L_{br}\,\cos(\theta_s-\alpha)}{\tau_r}\,i_b \\ \dot{\psi}_{dr} &= -\tfrac{1}{\tau_r}\,\psi_{dr} + \omega_s\,\psi_{qr} + \tfrac{L_m}{\tau_r}\,i_{ds} - \tfrac{L_{br}\,\sin(\theta_s-\alpha)}{\tau_r}\,i_b \\ J\,\dot{\omega}_r &= \tfrac{3\,P^2}{8}\Big[\tfrac{L_m}{L_r}\,(i_{qs}\,\psi_{dr} - i_{ds}\,\psi_{qr}) \\ &\quad + L_{bs}\,[\,\cos(\theta_s+\alpha)\,i_{ds} \\ &\quad - \sin(\theta_s+\alpha)\,i_{ds}\,]\,i_b\Big] - \tau_L, \end{aligned} \tag{13}$$

where $\tau_r = \frac{L_{lr}+L_{mr}}{r_r}$ is the rotor time constant, $\omega_r = \frac{2\,\omega_m}{P}$ is the rotor angular speed and $\omega_s = \omega_e - \omega_r$ is the slip angular speed.

Assuming now that the induction motor is fed by current inverters with fast current controllers and considering an IFOC scheme, the induction motor dynamics (13) reduces to

$$\begin{aligned}\dot{\psi}_{dr} &= -\tfrac{1}{\tau_r}\,\psi_{dr} + \tfrac{L_m}{\tau_r}\,i^*_{ds} - \tfrac{L_{br}}{\tau_r}\,\sin(\theta_s-\alpha)\,i_b\\ \dot{\theta}_r &= \omega_r\\ J\,\dot{\omega}_r &= \tfrac{3\,P^2}{8}\Big[\tfrac{L_m}{L_r}\,i^*_{qs}\,\psi_{dr} + L_{bs}\,[\,\cos(\theta_s+\alpha)\,i^*_{ds}\\ &\quad -\sin(\theta_s+\alpha)\,i^*_{qs}\,]\,i_b\Big] - \tau_L\\ \dot{\theta}_e &= \omega_r + \tfrac{L_m}{\tau_r}\,\tfrac{i^*_{qs}}{\psi_{dr}} - \tfrac{L_{br}}{\tau_r}\,\cos(\theta_s-\alpha)\,\tfrac{i_b}{\psi_{dr}}\end{aligned} \tag{14}$$

where i^*_{ds} and i^*_{qs} are the desired stator currents fixed by the current controllers.

To write the rotor flux dynamics (14) in terms of (6), first we identify the target and nuisance faults. Since we want to design a broken rotor bar detector that is not influenced by load conditions; τ_L and i_b in (14) are identified as the nuisance and target fault modes respectively, that is

$$l_n = \begin{bmatrix} 0\\ 0\\ \frac{-1}{J}\\ 0\end{bmatrix},\; l_t = \begin{bmatrix} -\frac{L_{br}}{\tau_r}\,\sin(\theta_s-\alpha)\\ 0\\ \frac{3P^2L_{bs}[\cos(\theta_s+\alpha)\,i^*_{ds}-\sin(\theta_s+\alpha)\,i^*_{qs}]}{8\,J}\\ -\frac{L_{br}}{\tau_r}\,\cos(\theta_s-\alpha)\,\frac{1}{\psi_{dr}}\end{bmatrix}.$$

Moreover, we have

$$\begin{aligned} f &= \begin{bmatrix} -\frac{1}{\tau_r}\,\psi_{dr} & \omega_r & 0 & \omega_r\end{bmatrix}^\top,\\ g &= \begin{bmatrix} \frac{L_m}{\tau_r} & 0 & 0 & 0\\ 0 & 0 & \frac{3\,P^2}{8\,J}\psi_{dr} & \frac{L_m}{\tau_r\,\psi_{dr}}\end{bmatrix}^\top.\end{aligned}$$

From a practical point of view, it is desirable to design a residual generator using the rotor speed, as it is an easily measurable state. However, it can be shown that with the rotor speed as the output of (14) the corresponding minimal unobservability distribution intersects the image of the nuisance fault signature, that is the load condition effects cannot be removed from the residual.

Note now that considering the rotor flux ψ_{dr} as the output of (14) the minimal unobservability distribution $\mathcal{S}^*$ is computed as

$$\mathcal{S}^* = \text{span}\left\{\begin{bmatrix} 0 & 0 & 0\\ \frac{1}{J} & 0 & 0\\ 0 & \frac{1}{J} & 0\\ \frac{1}{J} & 0 & 1\end{bmatrix}\right\}. \tag{15}$$

Thus, one has that (8) is satisfied for $\theta_s-\alpha\neq 0$ and we can go further to find the diffeomorphism (9). By inspection we note that (10), with $w_1 = y$, reads as

$$\begin{aligned}\dot{\psi}_{dr} &= -\tfrac{1}{\tau_r}\,\psi_{dr} + \tfrac{L_m}{\tau_r}\,i^*_{ds} - \tfrac{L_{br}}{\tau_r}\,\sin(\theta_s-\alpha)\,i_b\\ y &= \psi_{dr}\end{aligned} \tag{16}$$

and as a result we have that Problem 1 is solvable with the residual generator dynamics described by

$$\begin{aligned}\dot{\hat{\psi}}_{dr} &= -\Gamma\,\hat{\psi}_{dr} - \left(\tfrac{1}{\tau_r}-\Gamma\right)\,\psi_{dr} + \tfrac{L_m}{\tau_r}i^*_{ds}\\ r &= \hat{\psi}_{dr} - \psi_{dr},\end{aligned} \tag{17}$$

where $\Gamma > 0$. Furthermore, from the dynamics of r described by

$$\dot{r} = -\Gamma\,r + \frac{L_{br}}{\tau_r}\sin(\theta_s-\alpha)\,i_b, \tag{18}$$

it is possible to verify that conditions (i) and (ii) are satisfied as for $i_b = 0$ the residual goes exponentially to zero and is not affected by the nuisance fault (load torque). Moreover for $i_b \neq 0$ the residual will move away from zero.

Note that to compute the residual we need to have access to the rotor flux ψ_{dr} which is not always available. However, as it is used for monitoring purposes only, the rotor flux ψ_{dr} in (17) can be replaced by its steady state estimate given in [19] as

$$\psi_{dr} = \sqrt{\left[(L_sL_r - L_m^2)\left(i^{*2}_{ds}+i^{*2}_{qs}\right) - \frac{L_r}{\omega^*_e}(v_\beta i_\alpha - v_\alpha i_\beta)\right]}$$

where v_α, v_β are the stator voltages, i_α, i_β, are the rotor currents, $L_s = L_{ls}+L_{mr}$, $L_r = L_{lr}+L_{mr}$, $L_m = l_{mr}$ are the inductor motor inductances and ω^*_e is the excitation angular frequency (available from the IFOC scheme).

Now, we verify the performance of the broken rotor bar detector via numerical simulations. We consider a time variant load torque as in the table below.

Load torque	Motor 1 ($3HP$)	Motor 2 ($100HP$)
τ_L (Nm)	$10+2\,\cos(\theta_r)$	$80+10\,\cos(\theta_r)$

The residual behavior is shown in Figure 3. In order to verify that the residual is not affected asymptotically by changes on the load torque, at $t = 4$ sec, we reduce the constant component of load torque by $50\,\%$. Note that the residual is not asymptotically affected. Now to show that the residual actually detects the effect of broken rotor bars, at $t = 8$ sec we add the broken rotor bar winding. Note that the residual, as predicted, detects this effect.

As predicted by our computations the residual reacts to the target fault. However, note that if the rotor time constant is not exactly known deviations from the value used in the residual generator will produce a reaction of the fault detector. Since changes on the rotor time constant are mainly due to the rise of the temperature of the motor, the reaction of the fault detector to this mismatch should be slow. This problem also occurs in the Vienna Monitoring Method as it is assumed that the rotor time constant is exactly known. However, as adaptation schemes are generally used to estimate the rotor time constant this disadvantage of the proposed fault detector can be overcome. Noisy measurements can also disturb the detector's performance, however, initial observations indicate that it will be possible to distinguish between noisy measurements and broken rotor bar driven residuals.

Note that the limitations of the developed induction motor model affect the fault detector scheme. For instance, since we consider ideally distributed stator and rotor windings, it is not possible to determine the influence of other current harmonics on the residual.

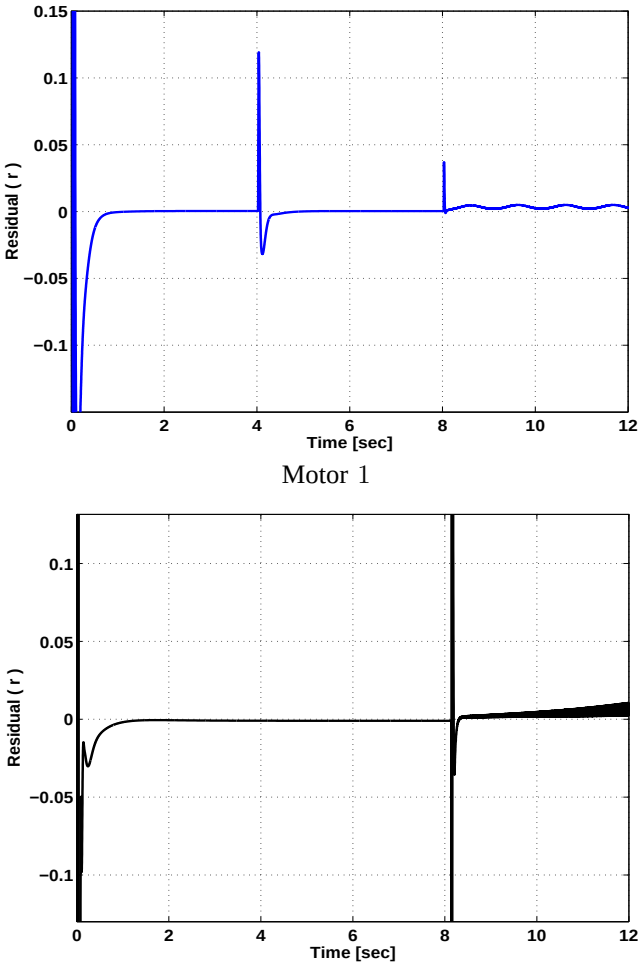

Fig. 3. Residual behavior.

V. CONCLUSION

We have developed a simplified model for a squirrel cage induction motor that includes broken rotor bars effects. Relying on differential geometry techniques, we have proposed a model-based solution to the broken rotor bar detection problem on IFOC driven squirrel cage induction motors. We show clearly that load torque conditions will not lead to errors in the detection as the fault detector is not affected by load torque. Numerical simulations of very different induction motors validate the model and the performance of the monitoring scheme.

VI. ACKNOWLEDGMENTS

The authors gratefully acknowledge the support of the NSF-ONR projects N00014-03-1-0344 and ECS-0224797. The first author would like to express his gratitude to Milun Perisic for helpful remarks.

REFERENCES

[1] W. T. Thomson and M. Fenger, Current Signature Analysis to Detect Induction Motor Faults, *IEEE Industry Applications Magazine*, July-August, pp. 26-34, 2001.

[2] M. H. Benbouzid and G. B. Kliman, What Stator Current Processing-Based Technique to Use for Induction Motor Rotor Fault Diagnosis? *IEEE Trans. on Energy Conversion*, 18(2), pp. 238-244, June 2003.

[3] E. Ritchie, X. Deng and T. Jokinen, Diagnosis of Rotor Faults in Squirrel Cage Induction Motors Using a Fuzzy Logic Approach, *Proc. Int. Conf. on Electr. Mach.*, Paris, France, pp. 348-352, 1994.

[4] F. Filippetti, G. Franchescini and C. Tassoni, Neural Network Aided On-line Diagnosis of Induction Motor Rotor Faults, *IEEE Trans. on Industrial Applications*, 31(4), pp. 892-899, 1995.

[5] J. F. Watson, S. Elder, Transient Analysis of the Line Current as a Fault Detection Technique for 3-phase Induction Motors, *Proc. Int. Conf. on Electr. Mach.*, pp. 1241-1245, 1992.

[6] R. Burnett, J. F. Watson and S. Elder, The Detection and Location of Rotor Faults Within Three Phase Induction Motors, *Proc. Int. Conf. on Electr. Mach.*, pp. 288-293, 1994.

[7] C. Kral, F. Pirker and G. Pascoli, Detection of Rotor Faults in Squirrel-Cage Induction Machines at Standstill for Batch Test by Means of the Vienna Monitoring Method, *IEEE Trans. on Industry Applications*, 38(3), pp. 618-624, May/June, 2002.

[8] M. Massoumnia, G. Verghese and A. Willsky, A., Failure Detection and Identification, *IEEE Trans. on Automatic Control*, 34(3), pp. 316-321, March 1989.

[9] M. Massoumnia, A Geometric Approach to the Synthesis of Failure Detection Filters, *IEEE Trans. on Automatic Control*, 31(9), pp. 339-346, September 1986.

[10] C. De Persis and A. Isidori, A Geometric Approach to Nonlinear Fault Detection and Isolation, *IEEE Trans. on Automatic Control*, 46(6), pp. 853-865, June 2001.

[11] S. Williamson and A. C. Smith, Steady-state analysis of 3-phase cage motors with rotor bar and end ring faults, *Proc. Inst. Elect. Eng.*, 2(3B), pp. 93-100, May 1982.

[12] ST. J. Manolas and J. A. Tegopoulos, Analysis of squirrel cage induction motors with broken bars and rings, *IEEE Trans. on Energy Conversion*, 14(4), pp. 1300-1305, December 1999.

[13] C. P. Krause, O. Wasynczuk and D. S. Sudho, **Analysis of Electric Machinery**, IEEE Press, New York, USA, 1995.

[14] R. Hirvonen, On-line condition monitoring of defects in squirrel cage motors, *Proc. Int. Conf. on Electr. Mach.*, 2, Paris, France, pp. 267-272, 1994.

[15] H. L. Jones, Failure Detection in Linear Systems, Ph.D. dissertation, MIT, Cambridge, 1973.

[16] R. V. Beard, Failure accommodation in linear systems through self-reorganization, Ph.D. dissertation, Dept. Aero. Astro., MIT, Cambridge, February 1971.

[17] H. Hammouri, M. Kinnaert and E.H. Yaagoubi, Fault Detection and Isolation for State Affine Systems, *European Journal of Control*, (4), pp. 2-16, 1998.

[18] R. Patton, P. Frank and R. Clark, **Fault Diagnosis in Dynamic Systems Theory and Application**, Prentice Hall International, First Edition, UK, 1989.

[19] M. Mijalkovic, Robust and Adaptive Control of Induction Motor Drives in Automotive Applications, Technical report, Northeastern University, May, 2002.